Available online at BCREC website: https://bcrec.id

Bulletin of Chemical Reaction Engineering & Catalysis, 15 (2) 2020, 514-524

Research Article

Sulfonated Hydrothermal Carbon-Based Catalyzed Esterification under Microwave Irradiation: Optimization and Kinetic Study

Laddawan Tumkot[1], Armando T. Quitain[2,3], Tetsuya Kida[2], Navadol Laosiripojana[4], Artiwan Shotipruk[1], Panatpong Boonnoun[5,*]

[1]Chemical Engineering Research Unit for Value Adding of Bioresources, Department of Chemical Engineering, Faculty of Engineering, Chulalongkorn University, Phayathai Road, Bangkok 10330, Thailand.
[2]Department of Applied Chemistry and Biochemistry, Faculty of Advanced Science and Technology, Kumamoto University, Kumamoto 860-8555, Japan.
[3]International Research Organization for Advanced Science and Technology, Kumamoto University, Kumamoto 860-8555, Japan.
[4]The Joint Graduate School of Energy and Environment, King Mongkut's University of Technology Thonburi, Prachauthit Road, Bangmod, Bangkok 10140, Thailand.
[5]Department of Industrial Engineering, Chemical Engineering Program, Faculty of Engineering, Naresuan University, Phitsanulok 65000, Thailand.

Received: 9th January 2020; Revised: 12th June 2020; Accepted: 13th June 2020; Available online: 30th July 2020; Published regularly: August 2020

Abstract

In this study, the esterification reaction of oleic acid (OA) with methanol was investigated in the presence of a sulfonated hydrothermal carbon-based catalyst under microwave irradiation. The reaction conditions were optimized using response surface methodology based on a central composite design. Three following variables were studied: methanol to OA molar ratios (2.5:1–7.5:1), reaction time (50–70 min) and catalyst loading (2–5 wt.%) to provide a statistical model with the coefficient of regression (R^2) of 0.9407. Based on the model, the optimum OA conversion of 95.6% was predicted at 5.8:1 methanol to OA molar ratio, 60 min and 3.05 wt.% catalyst loading. The experimental validation indicated that the model gave a good prediction of OA conversion (2.8% error). Furthermore, the reaction was found to be reasonably described by the pseudo-first order kinetics. The dependency of the reaction rate constant on temperatures gave a value of the activation energy of 64 kJ/mol.

Keywords: Carbon-based catalyst; Esterification; Microwave irradiation; Response surface methodology; Kinetic study

How to Cite: Tumkot, L., Quitain, A.T., Kida, T., Laosiripojana, N., Shotipruk, A., Boonnoun, P. (2020). Sulfonated Hydrothermal Carbon-Based Catalyzed Esterification under Microwave Irradiation: Optimization and Kinetic Study. *Bulletin of Chemical Reaction Engineering & Catalysis*, 15(2), 514-524 (doi:10.9767/bcrec.15.2.7040.514-524)

Permalink/DOI: https://doi.org/10.9767/bcrec.15.2.7040.514-524

1. Introduction

Owing to increasing global environment concerns, biodiesel, being a biodegradable fuel produced from renewable raw materials, such as vegetable oils and animal fats, is one of the most promising sources of alternative energy. It has good combustion, low toxicity and is compatible with petroleum diesel [1–3]. Considering the economic issue of the biodiesel production, raw materials and catalysts are two main contributing factors to the overall cost of biodiesel [4–6]. In this regard, low-cost feedstocks such as

* Corresponding Author.
E-mail: panatpongb@nu.ac.th (P. Boonnoun);
Telp: +66-55-4249, Fax: +66-55-964255

oils in high free fatty acids (non-edible seed oils and waste cooking oils), are more cost-effective raw materials for commercial biodiesel production. Free fatty acids (FFAs) in these low-cost raw materials are converted to biodiesel generally via acid-catalyzed esterification. Common acid catalysts are homogeneous catalysts, such as H_2SO_4, H_3PO_4, and HCl, which are the known causes of environmental problems and equipment corrosion [7].

Recently, heterogeneous carbon-based catalysts have been gaining attention owing to their high acid density and thermal stability, low corrosion, environmental friendliness, and their simple synthesis from low cost-carbon sources such as agricultural wastes. However, pyrolysis/carbonization method used in the conventional preparation of carbon-based catalysts has a major drawback in that it involves relatively high temperature (400–800 °C). Alternatively, when using hydrothermal carbonization process to synthesize carbonaceous materials, known as hydrothermal carbon (HTCs), the temperature is greatly reduced to approximately 150 – 250 °C. Furthermore, in the hydrothermal process, carbonization takes place in water, biomass with high moisture content can thus be carbonized, without expending considerable amount of the drying energy [8]. For use as catalysts, the prepared HTCs can be functionalized with a specific active site, using sulfonic acid, phosphate, polycyclic aromatic, polyethyleneimine, imidazole, and other acids to prepare catalyst for a particular reaction [9–14]. In a recent study, Zhang *et al.* [7] observed good reusability (after six uses) with a high catalytic performance for esterification of sulfonated carbon-based solid acid microspheric material prepared by the hydrothermal method.

Despite the advantages of the hydrothermally prepared catalysts, the reaction time for heterogeneous acid catalyzed esterification under conventional heating normally takes several hours [15,16]. Use of microwave (MW) irradiation instead of conventional heating has been shown to reduce reaction time of esterification from several hours to minutes [17,18]. Under microwave field, microwave absorbing materials are heated directly and selectively, making microwave heating rapid and uniform. Microwave heating has therefore found increasing number of applications including those with chemical reactions [19–22]. In microwave assisted carbon-based acid catalyzed biodiesel production, the carbon materials play double roles as catalyst and MW absorber [19].

This work aimed to study the esterification oleic acid (OA) with methanol using a hydrothermal carbon-based catalyst under MW irradiation. The reaction condition was optimized using response surface methodology (RSM) with a central composite design (CCD) to evaluate the effect of each variable (molar ratio of methanol to OA, reaction time and catalyst loading) and the variable interaction via a quadratic model. A statistical model was proposed and then experimentally validated at the suggested optimum condition. In addition, kinetic study of the OA esterification was performed to determine the kinetic parameters which would be important for future process design, including the reaction rate constants at different temperatures, the activation energy and the frequency factor.

2. Materials and Methods

2.1 Materials and Chemicals

The carbon precursor, D-glucose and sulfuric acid (laboratory grade, 98%) were purchased from Fluka, Singapore. Methanol (laboratory grade, 99% purity) was purchased from Wako, Japan. Oleic acid was purchased from Sigma-Aldrich, United States. The reference oleic acid methyl ester (OAME) standard and internal standard, 2,6-Dimethylnaphthalene (DMN) were purchased from GL Science Inc., Japan and Sigma-Aldrich, United States, respectively.

2.2 Preparation and Characterization of S-HTC

This research employed the previously described method of HTC synthesis [23]. The resulting HTC was functionalized using concentrated sulfuric acid to form the S-HTC. The physical and chemical characterization of the synthesized S-HTC was performed by elemental analysis (for C, H, N, S), Fourier-transformed infrared spectroscopy (FTIR), X-ray diffraction (XRD), thermogravimetric (TGA) and scanning electron microscopy (SEM) analyses, and the results were compared with those of HTC.

2.3 Esterification of OA and Methanol under MW Irradiation

The esterification of OA and methanol was used to test the catalytic activity of S-HTC. The reaction was performed using a microwave reactor (MARS6, CEM, USA) under a reaction temperature of 70–100 °C, reaction time of 50–70 min, methanol to OA molar ratio of 2.5:1–7.5:1 and catalyst loading of 1.5-3.5 by weight (wt%). The temperature in the control vessel was monitored by a thermocouple and that of

the other vessels by an infrared sensor. When the temperature reached the desire temperature, the microwave power is automatically cut off to maintain that temperature. In a typical run, OA, methanol and catalyst were firstly mixed and then irradiated at specified conditions. After the reaction, the system was cooled down automatically. The reaction products were discharged from the vessel and were allowed to settle into two phases. The top phase consisted of OAME and unreacted methanol, while the bottom phase was by-product of water. Unreacted methanol was removed by evaporation and then the OAME was drawn for the quantitative analysis by gas chromatography (GC–FID, Shimadzu, Japan) equipped with a flame ionization detector (FID) and a 5MS capillary column (0.25 mm × 0.25 mm × 30 m, Agilent Technologies, Inc., Japan). Helium was used as a carrier gas. The temperature of the injector and the detector were kept at 270 °C and 310 °C, respectively. A 20 mL aliquot of OAME sample was dissolved in 180 mL of n-hexane using DMN as the internal standard. The OA conversion was calculated from Equation (1);

$$\%Conversion = \frac{mol\ of\ OAME}{mol\ of\ OA} \times 100 \quad (1)$$

where OAME represents the quantification by GC-FID of OAME.

2.4 Design of Experiment, Analysis and Model fitting

The S-HTC catalyzed esterification was designed using RSM provided by Expert Design version 10 (Stat-Ease Inc. (2016), USA). A set of experiments was performed at a fixed temperature (100 °C) using pulsed MW to determine the influence of three parameters of the methanol to OA molar ratio (A), reaction time (B) and catalyst loading (C) and their interactions. Using CCD at three levels (low, middle and high), designated as –1, 0 and +1 respectively (Table 1), 17 experimental runs comprising eight factorial points, six axial points and three replicates at the center point, were performed. A quadratic model using regression analysis was fitted to the OA conversion values using both linear and non-linear forms. The conformity between experimental and predicted response of the model and the significance of the operating variables were evaluated based on the analysis of variance (ANOVA) and the regression coefficient (R^2).

Table 1. Levels of actual and coded factors.

Factors	–1	0	1
Molar ratio of methanol to OA (mol)	2.5	5	7.5
Reaction time (min)	50	60	70
Catalyst loading (wt%)	1.5	2.5	3.5

2.5 Kinetics Study of S-HTC Catalyzed Esterification

Esterification of OA with methanol, under the catalysis of S-HTC, produces OAME and water as shown in Equation (2). The rate of reaction strongly depends on temperature, and so the operating temperature in this study was varied between 70–100 °C under the previously determined optimized condition (methanol to OA molar ratio of 5.831:1 and catalyst loading of 3.047 wt.%) for 0, 15, 30, 45, and 60 min.

$$\underset{A}{Oleic\ acid} + \underset{B}{Methanol} \rightleftharpoons \underset{C}{Oleic\ methyl\ ester} + \underset{D}{Water} \quad (2)$$

A kinetic model was set up on the basis that the influence of the reverse reaction was negligible, due to the excess amount of methanol being used. The reaction rate equation was simplified to the first order pseudo-homogeneous equation, as shown in Equation (3);

$$-r = -\frac{dC_A}{dt} = kC_A \quad (3)$$

where C_A denotes the concentration of OA and k is forward reaction rate constant. For a constant volume system, X_A is a convenient term used in place of concentration of OA (C_A) and is expressed in Equation (4);

$$C_A = \frac{N_A}{V} = \frac{N_{AO}(1-X_A)}{V} = C_{AO}(1-X_A) \quad (4)$$

where N_{AO} and N_A are the initial molar amount and the molar amount of OA at later times, respectively. C_{AO} is the initial concentration of OA and V is the reaction volume.
Hence, Equation (3) becomes

$$-\frac{dC_A}{dt} = kC_{AO}(1-X_A) \quad (5)$$

The integrals of Equation (5) provides Equation (6),

$$-\ln(1-X_A) = kt \quad (6)$$

Thus, the rate constant, k, can be obtained by a linear fit of Equation (6). The activation energy can be calculated from the relation of rate constants at different temperatures by the Arrhenius equation, shown in Equation (7);

$$k = Ae^{-\frac{Ea}{RT}} \quad (7)$$

where A is the frequency factor and Ea is the activation energy. Linearization of Equation (7) becomes:

$$\ln k = -\frac{Ea}{RT} + \ln A \quad (8)$$

3. Results and Discussions

3.1 Characterization of S-HTC

The physicochemical characteristics of the HTC and the S-HTC catalyst are summarized in Table 2 and Figure 1. From the elemental analysis results in Table 2, it can be seen that the HTC derived from glucose had relatively high oxygen content (O/C ratio = 0.42). The increase in the oxygen content from the O/C ratio = 0.42 to 0.79 after sulfonation, indicated that the sulfonic acid group (–SO_3H) was successfully attached to the HTC to form S-HTC. The functionalization of sulfonic acid groups onto the prepared HTC was also verified by the sulfur content of the S-HTC, which was determined to be 1.36% on a mass basis by the elemental analysis. In addition, an increase in the total acidity, determined by titration method, was also observed for S-HTC. This value included both the weak (–COOH) and the strong (–SO_3H) acid sites. Despite the high acid density, the BET specific surface areas of both HTC and S-HTC were relatively low (<3 m^2/g), probably due to the low temperature of the hydrothermal carbonization process. The S-HTC had a slightly lower specific surface area than the HTC, which probably resulted from the particle

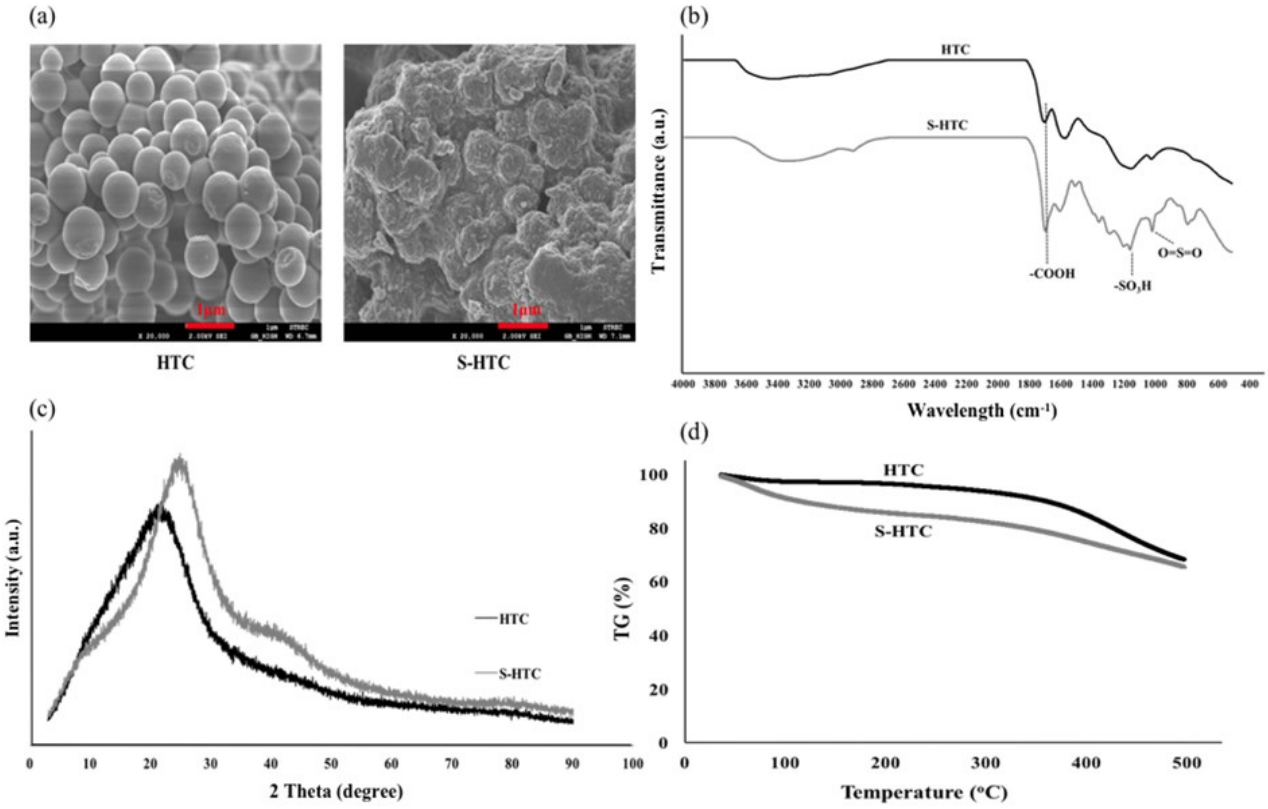

Figure 1. (a) SEM images of the HTC and S-HTC (b) FTIR spectrum (c) XRD pattern (d) TGA profiles.

Table 2. Physiochemical properties of HTC and S-HTC.

Sample	Elemental compositions				Atomic ratios		Surface area** (m^2/g)	Total acidity (mmol/g)
	%C	%H	%O*	%S	H/C	O/C		
HTC	66.31	5.96	27.73	N.D.	0.09	0.42	2.90	0.62
S-HTC	53.13	3.42	42.09	1.36	0.06	0.79	2.67	4.90

N.D. Not detected
*The oxygen composition was calculated by difference from 100% considering the other elements.
**BET surface area estimated from N_2 adsorption results.

agglomeration, as observed in the SEM image (Figure 1(a)).

The morphological structures of the HTC and S-HTC were observed by SEM, where the glucose-derived HTC particles have a typical spherical shape with the approximate size of 0.5 mm and tended to agglomerate into large particles (Figure 1(a)). The S-HTC was found to have a similar morphology but with a rougher surface. The FT-IR spectra (Figure 1(b)) confirmed the existence of sulfonic acid functional groups, with O=S=O symmetric stretching at 1020 cm^{-1} and $–SO_3H$ at 1167 cm^{-1} in the S-HTC after sulfonation of the HTC. Also, the absorbance at 1704 cm^{-1} revealed the presence of carboxylic acid groups. Thus, at least two types of Brønsted acid sites (sulfonic and carboxylic acid sites) were present in the prepared S-HTC, which are common acid sites found in carbon-based solid acid catalysts [24–26]. The XRD profiles of the HTC and S-HTC (Figure 1(c)) revealed broad C diffraction peaks (2θ = 10–30°) suggesting the amorphous structures of the samples [27].

The thermal stability of the sulfonic groups attached to the prepared S-HTC was evaluated by TGA analysis, with the results shown in Figure 1(d). From the TGA profile, HTC showed a weight loss of about 5% at around 250 °C, which corresponded to the loss of some functional groups (–OH mainly and some –COOH) [25], while the S-HTC showed a similar trend but with a slightly higher weight loss. Thus, the $–SO_3H$ groups on the surface of the S-HTC might be stable at temperatures as high as 250 °C before they start to deactivate from the carbon structure [28].

3.2 Optimization of the Conditions for the S-HTC Catalyzed Esterification of OA and Methanol

3.2.1 Quadratic regression model and variance analysis

The experimental operation of S-HTC catalyzed esterification of OA with methanol and the corresponding OA conversions (responses), as well as the model predicted results, are displayed in Table 3. The OA conversions ranged from 47.1% to 94.6%. The derived quadratic model, which includes all the independent variables and their binary interactions, is shown in Equation (9).

$$\begin{aligned} OA\ Conversion(\%) = & -62.44446 + 21.93250A \\ & + 1.27526B + 27.63576C - 0.078850AB \\ & - 0.38050AC + 0.17087BC - 1.30515A^2 \\ & - 0.00847B^2 - 5.66643C^2 \end{aligned} \quad (9)$$

where A, B and C are the actual values of the methanol to OA molar ratio, reaction time and

Table 3. CCD variables for S-HTC catalyzed esterification and experimental (response) and predicted percent OA conversions.

Experimental run	Methanol to OA molar ratio	Reaction time (min)	Catalyst loading (wt%)	Response % OA Conversion	Predicted % OA Conversion
1	2.5	50	1.5	59.7	55.4
2	7.5	50	1.5	78.4	73.0
3	2.5	70	1.5	68.8	58.8
4	7.5	70	1.5	76.3	77.8
5	2.5	50	3.5	75.0	68.7
6	7.5	50	3.5	86.4	82.9
7	2.5	70	3.5	87.5	80.4
8	7.5	70	3.5	94.6	96.0
9	0.8	60	2.5	47.1	47.0
10	9.2	60	2.5	85.5	74.9
11	5	43.1	2.5	83.4	82.0
12	5	76.8	2.5	90.5	96.0
13	5	60	0.8	60.2	61.9
14	5	60	4.2	86.5	88.7
15	5	60	2.5	91.9	91.5
16	5	60	2.5	93.4	91.5
17	5	60	2.5	90.0	91.5

catalyst loading, respectively. The coefficient of regression (R^2) was used to fit the data for the quadratic polynomial equation. Based on the obtained R^2 of 0.9407, the prediction of the response was able to cover more than 90% of the variability in the experiments. The satisfactory prediction of OA conversion based on regression model compared to the actual experimental data, is shown in Figure 2. The statistically significance of each parameter was evaluated by the analysis of variance (ANOVA) (as presented in Table 4). The significance of each term in Equation (9) was assessed by its corresponding p-value. At a 95% of confidence level (p-value < 0.05), A, C, A^2 and C^2 are significant factors. Moreover, the insignificant lack of fit confirmed that the quadratic model provided a satisfactory prediction of OA conversion.

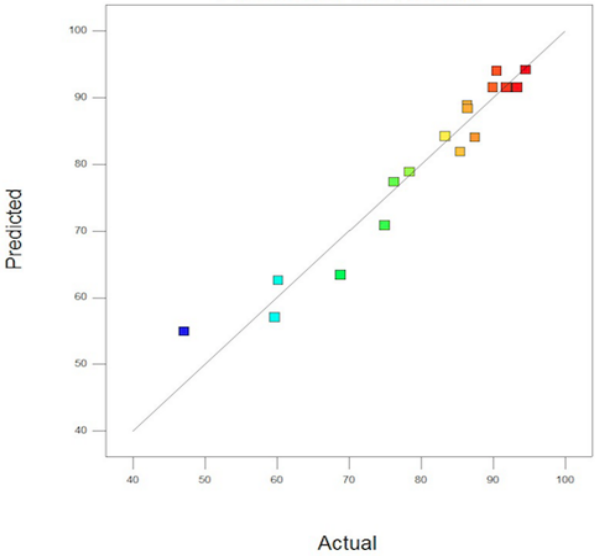

Figure 2. Comparison between the predicted and actual OA conversion.

3.2.2 Effect of variables on OA conversion

The effect of methanol to OA molar ratio, reaction time and catalyst loading on the OA conversion are presented as three-dimensional (3D) response surface plots in Figure 3. The lowest p-value of 0.0006 and the correspondingly largest F-value of 34.65 indicated that methanol to OA molar ratio was the most influential factor on OA conversion, followed by catalyst loading (Table 4).

The production of OAMEs was favored at a high methanol to OA molar ratio. In this equilibrium reaction, the excess methanol forces the reaction towards the production of OAME. This was also seen in the result of OA conversion, which increased as methanol to OA molar ratio from 2.5 to 7.5. The reaction time, on the other hand, showed an insignificant effect on OA conversion within the range studied (Figure 3(b,c)), whereas increasing the catalyst loading (wt.%) and hence the amount of catalysts, the Brønsted acid sites: (–SO_3H and –COOH), increased the OA conversion.

3.2.2 Effect of variables on OA conversion

The effect of methanol to OA molar ratio, re-

Table 4. Analysis of variance (ANOVA) for response surface quadratic model.

Source	Sum of Squares	Degree of freedom	Mean Square	F-value	p-value
Model	2801.16	9	311.24	12.35	0.0016*
A-Methanol to OA	873.33	1	873.33	34.65	0.0006*
B-Reaction time	115.80	1	115.80	4.59	0.0693
C-Catalyst loading	799.99	1	799.99	31.74	0.0008*
AB	31.09	1	31.09	1.23	0.3034
AC	7.24	1	7.24	0.29	0.6086
BC	23.36	1	23.36	0.93	0.3678
A^2	750.13	1	750.13	29.76	0.0010*
B^2	8.10	1	8.10	0.32	0.5886
C^2	361.97	1	361.97	14.36	0.0068*
Residual	176.43	7	25.20		
Lack of Fit	170.73	5	34.15	11.98	0.0788
Pure error	5.70	2			
Corrected total	4216.23	16			
R^2	0.9407				
Adj-R^2	0.8646				

*Parameters that significantly affect the reaction (p-value less than 0.05)

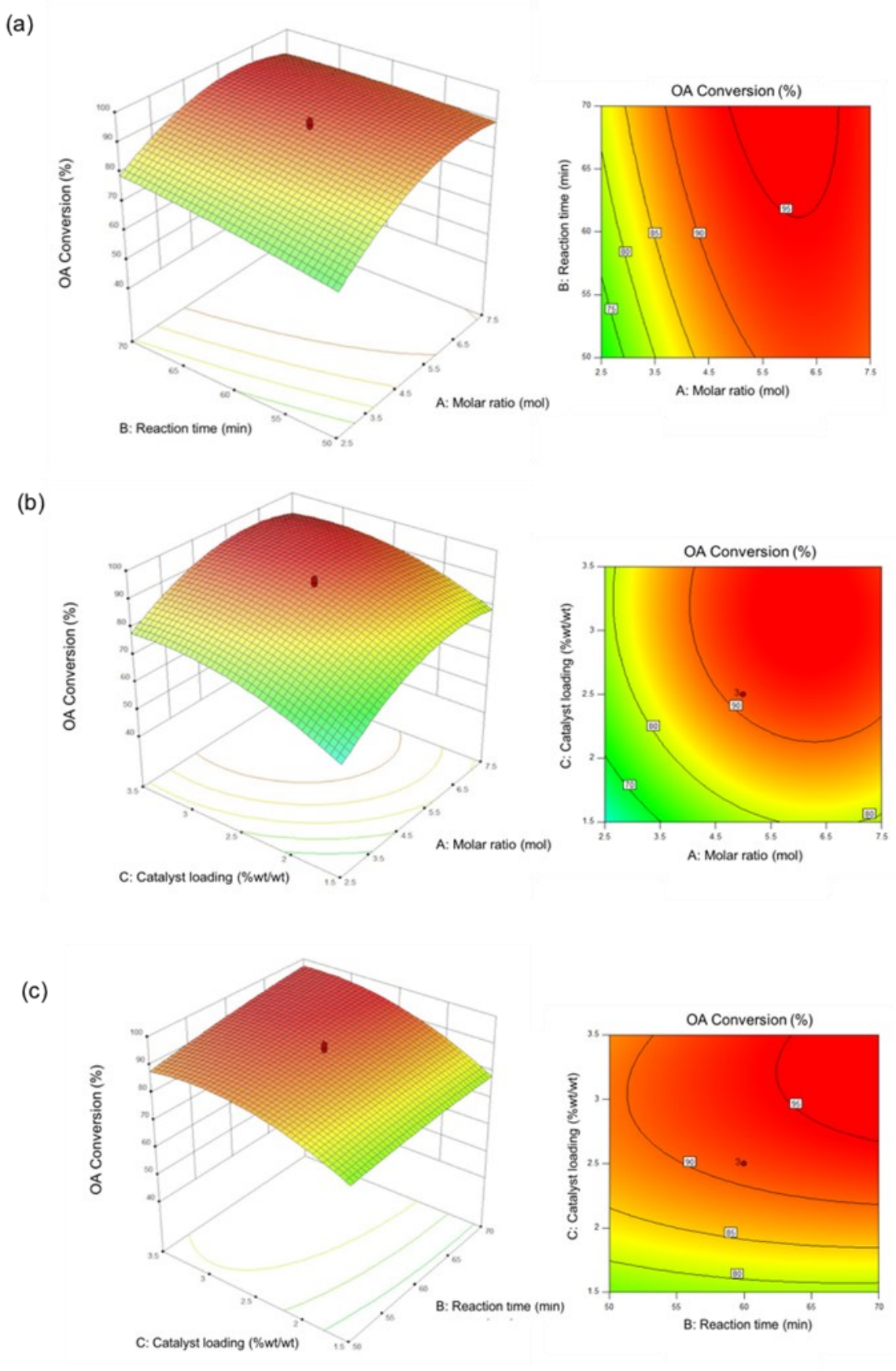

Figure 3. 3-D response surface and contour plots representing effects of pairs of variables: (a) methanol to OA and reaction time; (b) methanol to OA and catalyst loading; and (c) reaction time and catalyst loading, on OA conversion.

action time and catalyst loading on the OA conversion are presented as three-dimensional (3D) response surface plots in Figure 3. The lowest *p*-value of 0.0006 and the correspondingly largest *F*-value of 34.65 indicated that methanol to OA molar ratio was the most influential factor on OA conversion, followed by catalyst loading (Table 4).

The production of OAMEs was favored at a high methanol to OA molar ratio. In this equilibrium reaction, the excess methanol forces the reaction towards the production of OAME. This was also seen in the result of OA conversion, which increased as methanol to OA molar ratio from 2.5 to 7.5. The reaction time, on the other hand, showed an insignificant effect on OA conversion within the range studied (Figure 3(b,c)), whereas increasing the catalyst loading (wt.%) and hence the amount of catalysts, the Bronsted acid sites: (–SO_3H and –COOH), increased the OA conversion.

3.2.3 Optimization of OA conversion

RSM analysis provided the prediction of the optimal condition for OA conversion at a 5.831:1 methanol to OA molar ratio, a reaction time of 60 min and 3.05 wt.% catalyst loading to yield an expected 95.6% OA conversion. The accuracy of the model prediction was confirmed by experimental evaluation of the OA conversion under this RSM optimized condition and yielded an OA conversion of 92.8%, a 2.8% deviation from the model prediction. This result, therefore, suggested that the model is in good agreement with the experimental study. It should be noted also time taken for esterification of OA catalyzed hydrothermal carbon-based catalyst under MW heating in this study required shorter time compared with using conventional heating reported by Zhou *et al.* (60 min versus 120 min) [16].

Moreover, the carbon-based catalyst in the present work gave higher reactivity, compared with sulfated zirconia, for esterification of OA with methanol under MW heating. Specifically, Melo Junior *et al.* [29] reported considerable lower OA conversion (68.7%) obtained with sulfated zirconia after 20 min of reaction at 200 °C, OA to methanol ratio of 1:10, which could possibly be due to the lower acidity of sulfated zirconia (2.6 mmol/g versus 4.9 mmol/g). In addition, S-HTC in this work gave comparable reactivity compared with that prepared from wasted *flint* kaolin reported by Oliveira *et al.* [30], which gave 96.5% OA conversion after 40 min of reaction under MW heating at 115° and 1:60 of oleic acid: methanol molar ratio.

The reusability of S-HTC was also examined for esterification of OA under optimized reaction condition. The results showed that the OA conversion decreased by 50% after the first run. This decrease could be attributed to sulfur leaching and could be improved by regeneration of the spent catalyst with acid. Furthermore, the stability of the catalyst could be improved by modification of the catalyst synthesis that allow chemical bonding of the acid site (sulfonate group) to the carbon matrix.

3.3 Kinetics Study of the S-HTC Catalyzed Esterification Reaction

3.3.1 Determination of the kinetic parameters

To identify the kinetics of the reaction, experiments were carried out at different temperatures and times, with the results shown in Figure 4. The OA conversion increased with increasing reaction time. It should be noted that the OA conversion had already reached around 40% by the time the reaction system had reached the desired temperature (t = 0 min).

The reaction rate constant for respective temperatures was determined based on Equation (6) by plotting graph of ln (1–X_A) versus the reaction time (Figure 5), while Table 5 summarizes these values. High coefficient of determinations (R^2) were observed, and so the assumption of a pseudo-first order reaction rate was verified. The rate constants increased with the increasing reaction temperatures from 70 to 100 °C due to the endothermic reaction nature of the esterification reaction, suggesting

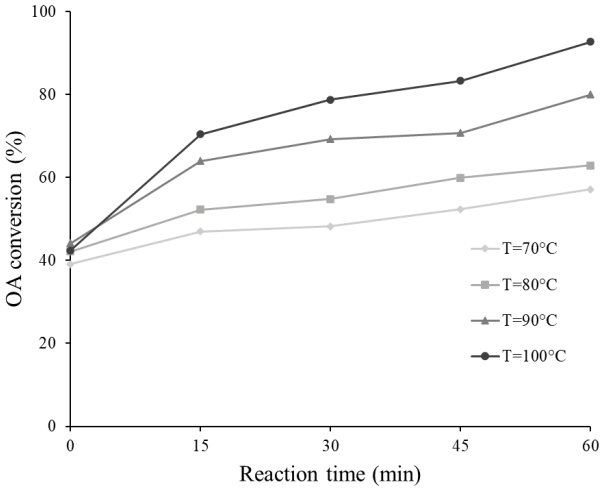

Figure 4. OA conversion as a function of time at different temperatures. [Conditions: methanol to OA molar ratio = 5.831:1, 3.047 wt% catalyst loading and microwave power set = 300 W].

that the forward reaction was accelerated by the increased reaction temperature.

3.3.2 Arrhenius plot and activation energy

The relation of ln k and 1/T was plotted to determine the activation energy and the frequency factor based on the Arrhenius equation, and is shown in Figure 6. The activation energy and frequency factor for the S-HTC catalyzed esterification of OA with methanol was found to be 64 kJ/mol and 2.58×10^7 min^{-1}, respectively. Note that the activation energy observed in the work was in the same range as those reported in the literature for the esterification reaction catalyzed by several acid compounds, such as: H_2SO_4, amino phosphonic acid resin, cation exchange resin/polyether sulfone, and NaY Zeolite, at 42–73 kJ/mol [31–34]. In addition, the value of frequency factor, representing the frequency of collisions between reactant molecules, observed in this work was 100–1000 times higher than the system of conventional heating [32], which correspond to the reduction of reaction time by MW heating compared to the conventional heating.

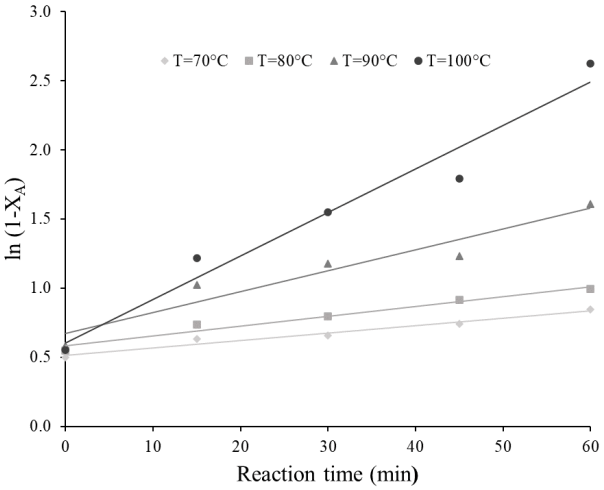

Figure 5. Kinetic plot for determination of reaction rate constants.

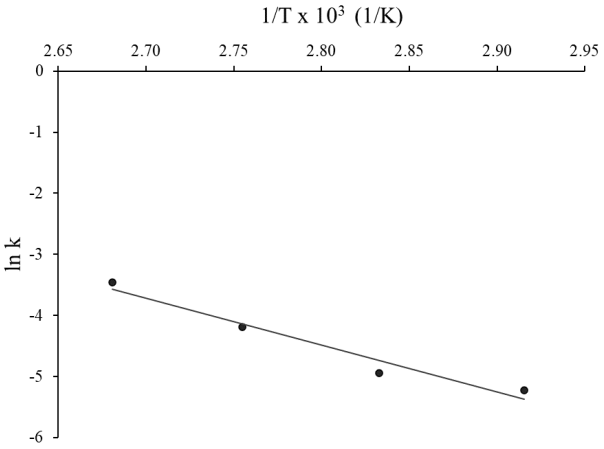

Figure 6. Arrhenius plot for estimation on activation energy and frequency factor.

4. Conclusions

A S-HTC catalyst was synthesized and used for the production of OAME from OA and methanol under MW irradiation. An RSM based on CCD was employed to predict and optimize the OA conversion of the of S-HTC catalyzed OA esterification with methanol. The optimum OA conversion of 95.6% was predicted at 5.8:1 methanol to OA molar ratio, 60 min and 3.05 wt% catalyst loading. The experimental validation indicated that the model gave good prediction of OA conversion, with only 2.8% error. Within the range of conditions studied, the methanol to OA molar ratio was the most influential factor on the OA conversion, followed by catalyst loading, whereas the reaction time showed a negligible effect. Compared with conventional heating employed in previous work, use of S-HTC catalyst coupled with MW irradiation in this study could result in the reduction of reaction time by half.

Acknowledgments

The authors gratefully acknowledge the financial supports of e-ASIA Joint Research Program (e-ASIA JRP), the Japan Student Services Organization (JASSO) Scholarship and the Thailand Science Research and Innovation (TSRI) (IRN62W0001).

References

[1] Ye, W., Gao, Y., Ding, H., Liu, M., Liu, S., Han, X., Qi, J. (2016). Kinetics of transesterification of palm oil under conventional heating and microwave irradiation, using CaO as heterogeneous catalyst. *Fuel*, 180, 574–579.

[2] Jiang, Y., Lu, J., Sun, K., Ma, L., Ding, J. (2013). Esterification of oleic acid with ethanol catalyzed by sulfonated cation exchange

Table 5. Reaction rate constants for S-HTC catalyzed OA esterification.

Temperature (°C)	Reaction rate constant, k (min^{-1})	Coefficient of determination (R^2)
70	0.0054	0.9627
80	0.0071	0.9654
90	0.0151	0.9246
100	0.0315	0.9598

resin: Experimental and kinetic studies. *Energy Conversion and Management*, 76, 980–985.

[3] Hashemzehi, M., Saghatoleslami, N., Nayebzadeh, H. (2017). Microwave-Assisted Solution Combustion Synthesis of Spinel-Type Mixed Oxides for Esterification Reaction. *Chemical Engineering Communications*, 204, 415–423.

[4] Chuah, L., Klemes, J., Yusup, S., Bokhari, A., Akbar, M. (2017). A review of cleaner intensification technologies in biodiesel production. *Journal of Cleaner Production*, 146, 181–193.

[5] Mardhiah, H., Ong, H., Masjuki, H., Lim, S., Lee, H. (2017). A review on latest developments and future prospects of heterogeneous catalyst in biodiesel production from non-edible oils. *Renewable and Sustainable Energy Reviews*, 67, 1225–1236.

[6] Trombettoni, V., Lanari, D., Prinsen, P., Luque, R., Marrocchi, A., Vaccaro, L. (2018). Recent advances in sulfonated resin catalysts for efficient biodiesel and bio-derived additives production. *Progress in Energy and Combustion Science*, 65, 136–162.

[7] Zhang, H., Luo, X., Li, X., Chen, G., He, F., Wu, T. (2016). Preparation and Characterization of a Sulfonated Carbon-based Solid Acid Microspheric Material (SCSAM) and its use for the Esterification of Oleic Acid with Methanol. *Austin Chemical Engineering*, 3, 1–6.

[8] Titirici, M., Antoniettia M., Baccile, N., (2008). Hydrothermal carbon from biomass: a comparison of the local structure from poly- to monosaccharides and pentoses/hexoses. *Green Chemistry*, 10, 1204–1212.

[9] Fraile, J., García-Bordejé, E., Roldán, L. (2012). Deactivation of sulfonated hydrothermal carbons in the presence of alcohols: Evidences for sulfonic esters formation. *Journal of Catalysis*, 289, 73–79.

[10] Nakajima, K., Hara, M. (2012). Amorphous Carbon with SO_3H Groups as a Solid Brønsted Acid Catalyst. *ACS Catalysis,* 2, 1296–1304.

[11] Fan, X., Yu, C., Ling, Z., Yang, J., Qiu, J. (2013). Hydrothermal Synthesis of Phosphate-Functionalized Carbon Nanotube-Containing Carbon Composites for Supercapacitors with Highly Stable Performance. *ACS Applied Materials & Interfaces*, 5, 2104−2110.

[12] Egres, A., Hatje, V., Miranda, D., Gallucci, F., Barros, F. (2019). Functional response of tropical estuarine benthic assemblages to perturbation by Polycyclic Aromatic Hydrocarbons. *Ecological Indicators*, 96, 229–240.

[13] Atta-Obeng, E., Dawson-Andoh, B., Felton, E., Dahle, G. (2018). Carbon Dioxide Capture Using Amine Functionalized Hydrothermal Carbons from Technical Lignin. *Waste and Biomass Valorization*, 10, 2725-2731.

[14] Demir-Cakan, R., Makowski, P., Antonietti, M., Goettmann, F., Titirici, M. (2010). Hydrothermal synthesis of imidazole functionalized carbon spheres and their application in catalysis. *Catalysis Today*, 150, 115–118.

[15] Theam, K.L., Islam, A., Lee, H.V., Taufiq-Yap, Y.H. (2015). Sucrose-derived catalytic biodiesel synthesis from low cost palm fatty acid distillate. *Process Safety and Environmental Protection*, 95, 126–135.

[16] Zhou, Y., Niu, S.L., Li, J. (2016). Activity of the carbon-based heterogeneous acid catalyst derived from bamboo in esterification of oleic acid with ethanol. *Energy Conversion and Management*, 114, 188–196.

[17] Lokman, I.M., Rashid, U., Taufiq-Yap, Y.H. (2015). Microwave-assisted methyl ester production from palm fatty acid distillate over a heterogeneous carbon-based solid acid catalyst. *Chemical Engineering & Technology*, 38, 1837–1844.

[18] Ning, Y., Niu, S. (2017). Preparation and catalytic performance in esterification of a bamboo-based heterogeneous acid catalyst with microwave assistance. *Energy Conversion and Management*, 153, 446–454.

[19] Menéndez, J.A., Arenillas, A., Fidalgo, B., Fernández, Y., Zubizarreta, L., Calvo, E., Bermúdez, J. (2010). Microwave heating processes involving carbon materials. *Fuel Processing Technology*, 91(1), 1–8.

[20] Mazo, P., Rios, L., Estenoz, D., Sponton, M. (2012). Self-esterification of partially maleated castor oil using conventional and microwave heating. *Chemical Engineering Journal*, 185–186, 347–351.

[21] Motasemi, F., Ani, F. (2012). A review on microwave-assisted production of biodiesel. *Renewable and Sustainable Energy Reviews*, 16, 4719–4733.

[22] Ma, L., Enmin, L., Du, L., Lu, J., Ding, J. (2016). Statistical modeling/optimization and process intensification of microwave-assisted acidified oil esterification. *Energy Conversion and Management*, 122, 411–418.

[23] Wataniyakul, P., Boonnoun, P., Quitain, A., Sasaki, M., Kida, T., Laosiripojana, N., Shotipruk, A. (2018). Preparation of hydrothermal carbon as catalyst support for conversion of biomass to 5-hydroxymethylfurfural. *Catalysis Communications*, 104, 41–47.

[24] Valle-Vigón, P., Sevilla, M., Fuertes, A. (2012). Sulfonated mesoporous silica–carbon composites and their use as solid acid catalysts. *Applied Surface Science*, 261, 574–583.

[25] Pileidis, F., Tabassum, M., Coutts, S., Titirici, M. (2014). Esterification of levulinic acid into ethyl levulinate catalysed by sulfonated hydrothermal carbons. *Chinese Journal of Catalysis*, 35, 929–936.

[26] Tran, T., Kaiprommarat, S., Kongparakul, S., Reubroycharoen, P., Guan, G., Nguyen, M., Samart, C. (2016). Green biodiesel production from waste cooking oil using an environmentally benign acid catalyst. *Waste Management*, 52, 367–374.

[27] Malins, K., Kampars, V., Brinks, J., Neibolte, I., Murnieks, R. (2015). Synthesis of activated carbon based heterogenous acid catalyst for biodiesel preparation. *Applied Catalysis B: Environmental*, 176–177, 553–558.

[28] Liu, T., Li, Z., Li, W., Shi, C., Wang, Y. (2013). Preparation and characterization of biomass carbon-based solid acid catalyst for the esterification of oleic acid with methanol. *Bioresource Technology*, 133, 618–621.

[29] Oliveira, A.N., Costa, L.R.S.C., Pires, L.H.O.P., Nascimento, L.A.S., Angélica, R.S., Costa, C.E.F.C., Zamian, J.R., Filho, G.N.R. (2013). Microwave-assisted preparation of a new esterification catalyst from wasted *flint* kaolin. *Fuel*, 103, 626–631.

[30] Melo Junior, C.A.R., Albuquerque, C.E.R., Carneiro, J.S.A., Dariva, C., Fortuny, M., Santos, A.F., Egues, S.M.S., Ramos, A.L.D. (2010). Solid-Acid-Catalyzed Esterification of Oleic Acid Assisted by Microwave Heating. *Industrial & Engineering Chemistry Research*, 49, 12135–12139.

[31] Liu, W., Yin, P., Liu, X., Chen, W., Chen, H., Liu, C., Qu, R., Xu, Q. (2013). Microwave assisted esterification of free fatty acid over a heterogeneous catalyst for biodiesel production. *Energy Conversion and Management*, 76, 1009–1014.

[32] Lieu, T., Yusup, S., Moniruzzaman M., (2016). Kinetic study on microwave-assisted esterification of free fatty acids derived from Ceiba pentandra Seed Oil. *Bioresource Technology*, 211, 248–256.

[33] Zhang, H., Ding, J., Qiu, Y., Zengdian Z. (2012). Kinetics of esterification of acidified oil with different alcohols by a cation ion-exchange resin/polyethersulfone hybrid catalytic membrane. *Bioresource Technology*, 112, 28–33.

[34] Abbas, A., Abbas, S. (2013). Kinetic Study and Simulation of Oleic Acid Esterification in Different Type of Reactors. *Iraqi Journal of Chemical and Petroleum Engineering*, 14, 13–20.